First-principles study of lithium-doped carbon clathrates under pressure

2008 J. Phys.: Condens. Matter 20 215218

(http://iopscience.iop.org/0953-8984/20/21/215218)

J. Phys.: Condens. Matter **20** (2008) 215218 (7pp) doi:10.1088/0953-8984/20/21/215218

First-principles study of lithium-doped carbon clathrates under pressure

Nicolas Rey[1], **Alfonso Muñoz**[2,3], **Placida Rodríguez-Hernández**[2,3] **and Alfonso San Miguel**[1]

[1] Laboratoire de Physique de la Matière Condensée et Nanostructures, Université Lyon 1; CNRS, UMR 5586, F-69622 Villeurbanne, France
[2] Departamento de Fisica Fundamental II, Universidad de La Laguna E38205 La Laguna, Tenerife, Spain

E-mail: amunoz@ull.es and alfonso.san.miguel@lpmcn.univ-lyon1.fr

Received 5 January 2008, in final form 17 March 2008
Published 22 April 2008
Online at stacks.iop.org/JPhysCM/20/215218

Abstract

We present a theoretical study of the behavior under pressure of the two hypothetical C_{46} and Li_8C_{46} type-I carbon clathrates in order to obtain new information concerning their synthesis. Using *ab initio* calculations, we have explored the energetic and structural properties under pressure of these two carbon based cage-like materials. These low-density metastable phases show large negative pressure transitions compared to diamond, which represent a serious obstacle to their synthesis. However, we show that a minimum energy barrier can be reached close to 40 GPa, suggesting that synthesis of the Li-clathrate under extreme conditions of pressure and temperature may be possible. The electronic band structure with related density of states behavior under pressure, as well as the dependence of the active Raman modes with pressure are also examined.

(Some figures in this article are in colour only in the electronic version)

1. Introduction

Hypothetical carbon analogues to silicon clathrates are predicted to exhibit promising properties of fundamental and technological interest. This low-density class of cage-like materials, related to the zeolite topology, were first investigated by Nesper *et al* [1]. They allow the intercalation of guest atoms inside the cages and therefore display unique properties. Exceptional values for mechanical properties or superconductivity at high temperature are predicted within the framework of *ab initio* calculations [1–4]. Also the low work function of the metallic Li_8C_{46} clathrate would be interesting for the design of potential electron-emitting devices [5]. Contrary to the other group-14 clathrates (Si, Ge and Sn), the synthesis of carbon clathrates remains a challenge, although the deposition of C_{20} or C_{36} networks, the basic units of which have a comparable size to those of the carbon clathrates, have been prepared [6, 7].

Type-I semiconducting carbon clathrates consist of the assembly of face-sharing C_{20} and C_{24} nano-cages, resulting in a cubic structure (SG: $Pm\bar{3}n$, No 223) (figure 1). They would represent a low-density fourfold diamond-like sp^3 configuration. Intercalation with Li and Be small atoms inside each cage of the type-I carbon clathrate has been suggested [8]. *Ab initio* calculations indicate that upon efficient doping carbon clathrates would turn metallic [2, 5, 9–11]. Furthermore, large values of the electron–phonon interaction potential allow us to envisage carbon clathrates as possible candidates for high-temperature superconductivity [4, 9, 11]. Recently, Zipoli *et al* have calculated a large value of electron–phonon coupling for the clathrate FC_{34}, leading to a superconducting temperature close to 77 K [12]. In addition, Blase *et al* have shown that the minimum strength of the carbon clathrates should be larger than that of diamond [3]. Carbon clathrates have also been predicted to have extraordinary mechanical properties, such as a bulk modulus close to that of diamond [2, 13] or even high strength limits under tension and shear beyond those of diamond [3].

The silicon type-I clathrate Ba_8Si_{46} can be synthesized from a precursor consisting of a stoichiometric mixture of $BaSi_2$ and Si at 3 GPa and 800 °C [14]. An attempt was

[3] MALTA Consolider Ingenio 2010 team.

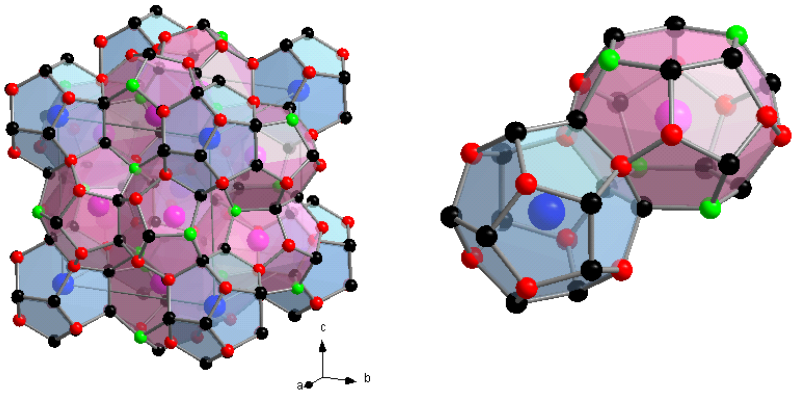

Figure 1. Crystal structure of type-I Li_8C_{46} clathrate (SG: $Pm\bar{3}n$, No 223). The white solid lines show the cubic unit cell. A detail of the two building polyhedrons consisting of two nano-cages of 20 atoms (C_{20} cage) and 24 atoms (C_{24} cage) are respectively represented in dark- and light-grey. The nano-cages are formed of carbon atoms occupying the following Wyckoff positions identified with different colors: C(1) 6c (light grey), C(2) 16i (dark grey) and C(3) 24k (black). The Li guest atoms inserted inside the cages occupy the positions Li(1) 2a (black) and Li(2) 6d (grey). (Color online version: the different Wyckoff positions are identified with different colors.)

made by Yamanaka *et al* to prepare a carbon clathrate using high-pressure (HP) and high-temperature (HT) conditions from the polymerization of C_{60} but no evidence of a clathrate-like phase analogous to Si-clathrates was found [15]. Another possible HPHT route has been envisaged using a Li–graphite intercalation compound, where the Li atoms could frustrate the graphite–diamond conversion and promote the formation of the endohedrally doped nano-cages [13, 16]. This idea is supported by the observation of the half conversion of the sp^2 bonds into sp^3 bonds at 17 GPa when graphite is pressurized [17].

In this work, we investigate the high-pressure properties of the C_{46} and Li_8C_{46} carbon clathrates within the framework of density functional theory as a way to obtain new information concerning their synthesis. The diamond–clathrate transition is discussed as well as the prospect of a reaction path leading to Li-intercalated carbon clathrates. The electronic band structure properties of C_{46} and Li_8C_{46} under pressure are also examined. We have calculated the active Raman modes of Li_8C_{46} and studied their pressure dependence which could contribute to the identification of carbon clathrate crystals if synthesized for instance in a diamond anvil cell.

2. Computational details

Our *ab initio* calculations were performed with the VASP code [18], using the projector augmented waves (PAW) [19] pseudopotentials supplied with the package [20], within the generalized gradient approximation (GGA) for the exchange–correlation energy [21]. This choice is justified, because for sp^3 carbon based materials GGA gives a better evaluation of the C–C distance [22, 23]. A plane-wave energy cut-off of 650 eV together with a $(4\times4\times4)$ Monkhorst–Pack grid corresponding to 10 k-points in the irreducible part of the Brillouin zone were used for the C_{46} and Li_8C_{46} compounds. Our k-mesh was enough to reach convergence due to the large clathrate cells. Thus, convergence of 2 meV/atoms in the difference of total energies and 0.2 GPa in pressure was reached. The cell and internal parameters were fully relaxed in order to obtain forces over the atoms lower than 0.005 eV $Å^{-1}$. The resulting energies as a function of the volume were fitted using a Murnaghan equation of state (EOS) [24] to obtain the equilibrium volume, the bulk modulus and its pressure derivative at zero pressure. The calculated pressure values are in excellent agreement with those provided from the fit. The study of the enthalpy allowed us to determine the relative stable phase.

Table 1. Structural and cohesive parameters of diamond (C_2), C_{46} and Li_8C_{46}. The equilibrium volume V_0 and cell parameter a_0 are obtained after relaxation of the forces. The bulk modulus B_0 and its pressure derivative B_0' are obtained with the Murnaghan EOS fit. The relative atomic volume V/V_0 and enthalpy ΔH_0 with respect to the diamond phase are also given.

	a_0 (Å)	V_0 (Å^3)	V/V_0	B_0 (GPa)	B_0'	ΔH_0 (eV/atom)
C_2	3.576	11.4	1.000	437	3.22	0.00
	3.567[a]			442[b]		
C_{46}	6.696	300.2	1.145	371	3.44	0.09
Li_8C_{46}	6.833	319.0	1.035	356	3.13	1.48

[a] Experimental value from [26].
[b] Experimental value from [25].

3. Results

3.1. Structural properties

Figure 2 shows the calculated energy–volume (E–V) curves of the carbon phases considered, i.e. diamond (C_2) which is included for comparison and the C_{46} and Li_8C_{46} clathrates structures. The diamond phase has the lowest energy and is the most stable at zero pressure. In table 1, the results for the three studied structures are given from our calculations together with existing experimental values. The internal parameters of the equilibrium volume of C_{46} and Li_8C_{46} are shown in table 2. Our calculated values for the lattice

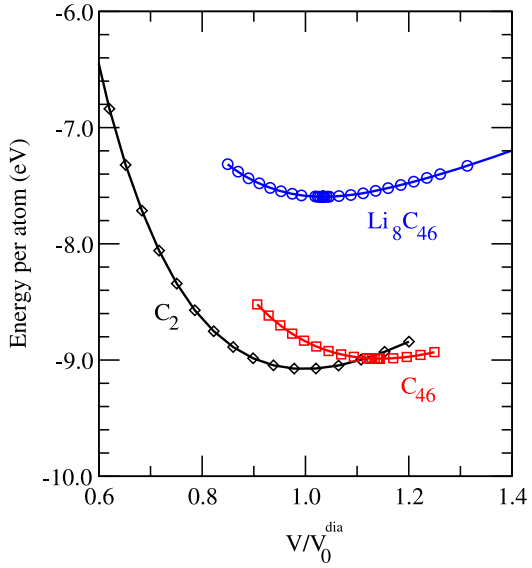

Figure 2. Calculated energy–volume curves for diamond (C_2), C_{46} and Li_8C_{46}. V_0^{dia} is the atomic volume of the diamond structure at equilibrium.

Table 2. Internal parameters of the C_{46} and Li_8C_{46} clathrates at their equilibrium volume.

Atoms	Wyckoff positions	Internal parameters (x, y, z)		
C_{46}, SG: $Pm\bar{3}n$, No 223, $Z = 1$				
C (1)	6c	0.25		0.5
C (2)	16i (x, x, x)	0.1845	0.1845	0.1845
C (3)	24k (0, y, z)	0	0.3056	0.1187
Li_8C_{46}, SG: $Pm\bar{3}n$, No 223, $Z = 1$				
C (1)	6c	0.25	0	0.5
C (2)	16i (x, x, x)	0.1854	0.1854	0.1854
C (3)	24k (0, y, z)	0	0.0345	0.1213
Li (1)	2a	0	0	0
Li (2)	6d	0.25	0.5	0

parameter and the bulk modulus of diamond are in excellent agreement with the experimental works [25, 26]. The resulting equilibrium lattice parameter and bulk modulus for C_{46} (a = 6.696 Å, B_0 = 371 GPa) are close to those from previous LDA and GGA studies [5, 12]. The intercalation of Li atoms at the center of the C_{20} and C_{24} cages leads to an expansion of the lattice parameter (a = 6.833 Å) as well as a higher compressibility (B_0 = 356 GPa). The atomic volume has been slightly expanded by 14.5% and 3.5% for the C_{46} and the Li_8C_{46} phases, respectively, with respect to diamond. We find an energy difference of 92 meV/atom for C_{46} relative to diamond, in good agreement with Nesper *et al* (90 meV/atom) [1] who also used the PAW method. Other *ab initio* methods give much higher energy differences of 144–210 meV/atom [27–30]. Despite the discrepancies found from all the mentioned calculations, it is remarkable that these binding energies, relative to diamond, are considerably lower than that of the fullerene C_{60} (430 meV/atom) [31]. However, according to our calculations, filling the voids inside the C_{46} clathrate dramatically increases the enthalpy at zero pressure to 1.48 eV/atom.

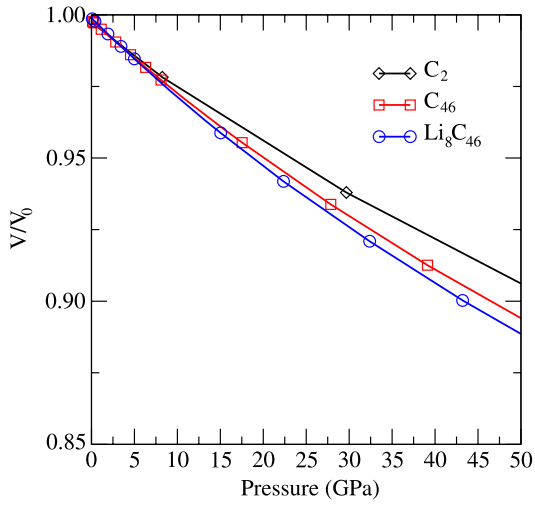

Figure 3. Variation of volume as a function of pressure for diamond (C_2), C_{46} and Li_8C_{46}.

The compressibility of the C_{46} and Li_8C_{46} clathrates is close to that of diamond until ∼8 GPa (figure 3). Then C_{46} and Li_8C_{46} become slightly more compressible than diamond, the pure clathrate being less compressible than the filled clathrate. This contrasts with the observations in Si-clathrates [32] in which intercalation trends to shift the bulk modulus towards the Si-diamond phase. The pressure-evolution of the C–C and Li–C distances in the cages of the two clathrates are displayed in figure 4. The insertion of lithium inside each cage of C_{46} leads to a slight extension of the cages and produces a general stiffening in the pressure-evolution of the C–C distances. The Li–C and C–C distances decrease smoothly with pressure. There is no sudden drop corresponding to a reduction in cell volume as has been experimentally observed in the Ba–Si and Si–Si distances of Ba_8Si_{46} [33, 34].

3.2. Stability under pressure

The diamond structure is the most stable phase studied in this work for positive pressures (figure 5). Enthalpy curves of C_{46} and Li_8C_{46} are found to be lower than that of diamond at −19 and −187 GPa, respectively. Our $C_2 \rightarrow C_{46}$ pressure transition agrees reasonably with the one calculated by Perottoni and Da Jornada within a Hartree–Fock approximation [30]. Negative pressure values are expected in those kinds of transition, implying expanded phases compared to diamond. Although, in absolute values, they are much larger than those calculated in the case of the $Si_2 \rightarrow Si_{46}$ (−6 GPa) [30] and $Ge_2 \rightarrow Ge_{46}$ (−2.4 GPa) [35] transitions. In the case of the intercalated type-I carbon clathrates with Na (P_t = −77 GPa) [30] or Li, huge negative pressure transitions relative to diamond seem to be systematic and render observation of the doped clathrate phases difficult.

In order to estimate the phase stability of Li_8C_{46}, we considered the following reaction:

$$8Li + 23C_2 \rightarrow Li_8C_{46}, \quad (1)$$

involving a stoichiometric ratio of metallic Li and diamond (C_2) to obtain the Li_8C_{46} compound. Thus, we studied the

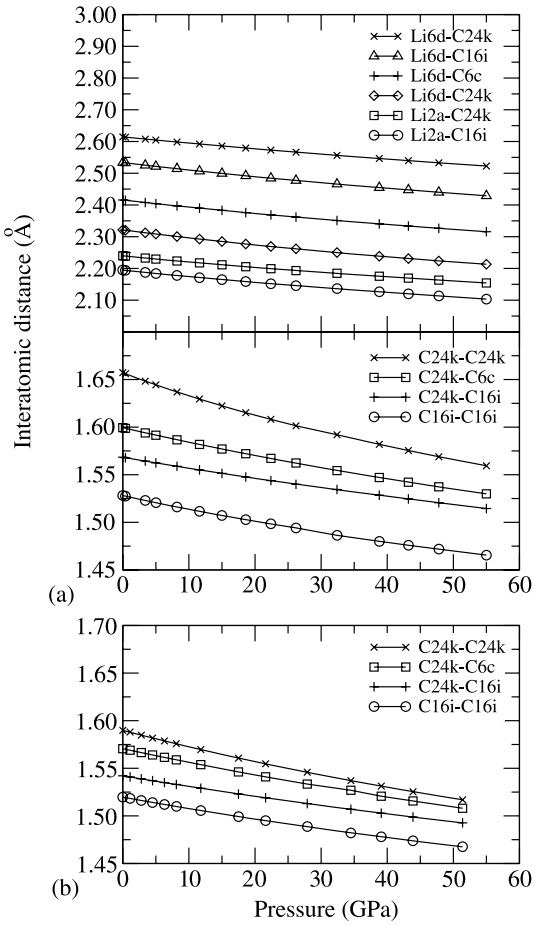

Figure 4. Top: evolution of interatomic distances with pressure for Li_8C_{46} (a): Li–C (top panel) and C–C distances (bottom panel), and for C_{46} (b): C–C distances.

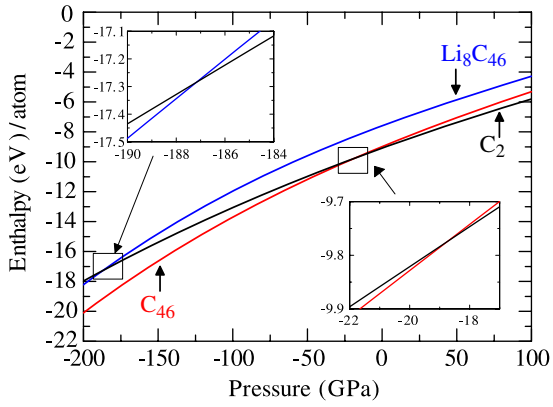

Figure 5. Enthalpies of the diamond (C_2) and the C_{46} and Li_8C_{46} clathrate phases as a function of pressure. The insets provide a zoom of the regions of interest.

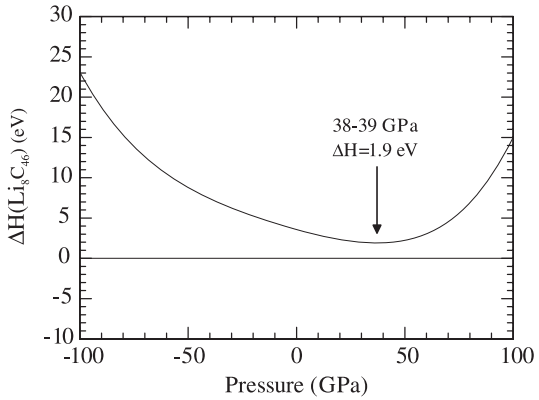

Figure 6. Relative enthalpy of Li_8C_{46} from equation (2) as a function of pressure. $\Delta H(Li_8C_{46}) > 0$ for the pressure range studied. A minimum corresponding to an energy barrier of 1.9 eV is found at 38–39 GPa.

variation of enthalpy of the previous reaction, defined as follows:

$$\Delta H(Li_8C_{46}) = H(Li_8C_{46}) - 8H(Li) - 23H(C_2). \quad (2)$$

Figure 6 shows the variation of $\Delta H(Li_8C_{46})$ as a function of the pressure. $\Delta H(Li_8C_{46})$ is always positive, indicating that the considered reaction (equation (1)) is not favorable in the pressure range studied. However, we have found a minimum corresponding to an energy barrier of 1.9 eV around 38–39 GPa.

3.3. Electronic properties under pressure

We have calculated the electronic band structure of pure and doped carbon clathrates choosing the same path along the same high-symmetry directions of the Brillouin zone as in reference [41]. The band structure of the semiconducting C_{46} at zero pressure and at 51.3 GPa is provided in figures 7(c) and (d). We find a quasi-direct band gap of approximately 3.88 eV at zero pressure between Γ–X, which is in good agreement with previously reported results [5, 36]. The band gap value decreases with pressure, reaching 3.69 eV at 51.3 GPa, and becomes direct from 2.8 GPa. We can check in figure 7(a) that the intercalation of lithium in each cage of C_{46} leads to metallic behavior with the filling of the conduction band by Li 2s electrons. A maximum in the density of states at the Fermi level E_F is observed, suggesting interesting superconducting properties as previously remarked [2, 4, 5, 11]. No dramatic changes were found at 55 GPa in the band structure of Li_8C_{46}, especially in the conduction band in the vicinity of E_F (figure 7(d)). In this regard, a band crossing over the Fermi level in the conduction band of Ba_8Si_{46} near the R-point, ascribed to an electronic topological transition, has been calculated recently [34]. In Li_8C_{46}, the Fermi energy is found to increase with pressure, corresponding to a shift of $\Delta E_F \approx 1.7$ eV between 0 and 55 GPa. This indicates that the pressure is a valuable parameter for tuning the charge transfer in these guest–host systems. We point out that the density of states around E_F present a maximum at 55 GPa.

3.4. Dynamical properties of Li_8C_{46} under pressure

We used the direct approach based on the small displacements to calculate the eigenvalues of the dynamical matrix at the Γ-point of the Brillouin zone [39, 40]. In order to achieve

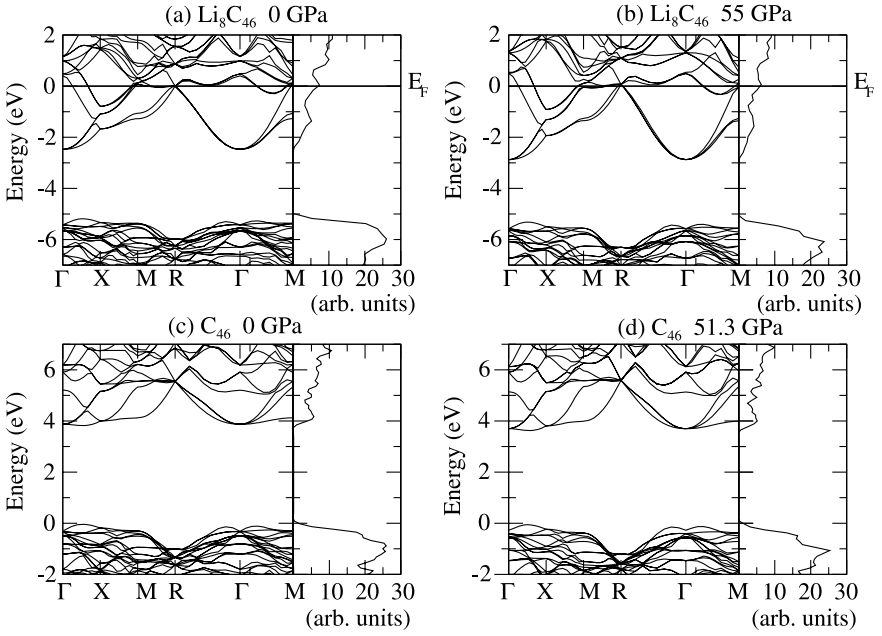

Figure 7. Band structure and density of states associated with Li_8C_{46} at 0 GPa (a) and at 55 GPa (b) and for C_{46} at 0 GPa (c) and at 51.3 GPa (d). In the case of the Li_8C_{46} metallic compound, the Fermi energy is taken as reference. In the semiconducting C_{46}, the top of the valence band is chosen as the energy reference.

Table 3. Raman active modes of Li_8C_{46} (point group: O_h) for the equilibrium volume (at the Γ-point). The frequency at 870 cm^{-1} consists of the combination of a Raman (R) and an infra-red (IR) mode. These frequencies and their representation were calculated with the PHONON program [37].

Representation	Frequency (cm^{-1})	Activity
T_{2g}	247	R
E_g	310	R
E_g	387	R
T_{2g}	425	R
E_g	550	R
T_{2g}	649	R
E_g	654	R
A_{1g}	674	R
E_g	690	R
T_{2g}	766	R
E_g	804	R
T_{2g}	813	R
T_{2g}	864	R
$A_{1g} + T_{1u}$	870	R + IR
T_{2g}	921	R
E_g	944	R
T_{2g}	959	R
E_g	976	R
T_{2g}	1049	R
A_{1g}	1080	R

accurate results, we relaxed the cell and the internal parameters to obtain forces over the atoms below 0.0001 eV $Å^{-1}$. We performed our study with the PHON [38] and PHONON [37] programs using a (1 × 1 × 1) supercell. In order to obtain well-converged results we tested different small displacements, and a (4 × 4 × 4) *k*-mesh was used to reach convergence of the phonon frequencies lower than 3–4 cm^{-1}.

In order to link our theoretical results with possible future Raman spectroscopy measurements, if synthesized, we present

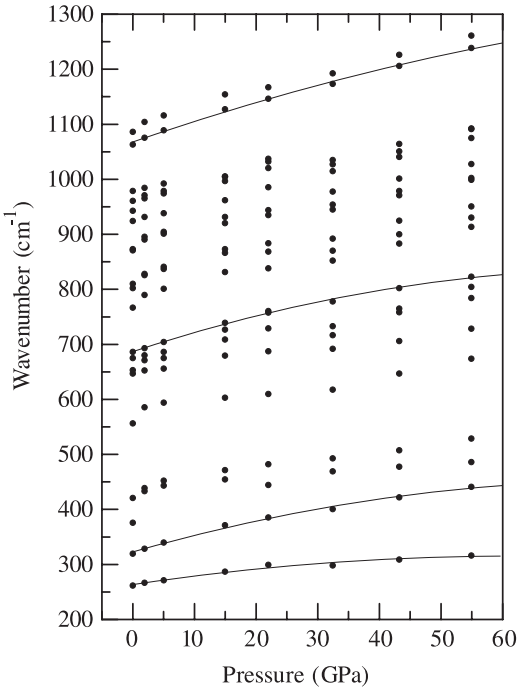

Figure 8. Pressure-evolution of the calculated Li_8C_{46} Raman frequencies with the PHON program [38]. The continuous lines represent a polynomial fit (see table 4).

a list of the active Raman modes of the Li_8C_{46} clathrate corresponding to the equilibrium volume in table 3, which could be helpful as a reference for the experimental study.

Figure 8 shows the evolution with pressure of the calculated Raman frequencies obtained with the PHON program [38]. We point out that a typical discrepancy of

Table 4. Coefficients of the pressure dependence of Li_8C_{46} Raman frequencies shown in figure 8. A second-order polynomial function was used to fit the calculated frequencies.

$\nu(P) = a + b\ P + c\ P^2$				
	T_{2g}	E_g	E_g	T_{2g}
a (cm^{-1})	263.28	322.83	686.84	1067.68
b (cm^{-1} GPa^{-1})	1.69	3.18	3.68	3.87
c (cm^{-1} GPa^{-2})	1.39×10^{-2}	1.95×10^{-2}	2.26×10^{-2}	1.45×10^{-2}

15 cm^{-1} between the eigenvalues calculated from the two programs PHON and PHONON was observed. This value can be considered as an average uncertainty of our calculated frequencies. The pressure dependence of some frequencies can be reproduced with a second-order polynomial fit as shown with the continuous lines in the figure. For the other frequencies, a more complicated behavior is observed. In that case, we can distinguish three regimes with different effective slopes.

4. Summary and conclusions

In this work we have presented an *ab initio* theoretical study of the behavior under pressure of the C_{46} and Li_8C_{46} carbon clathrates. We have analyzed the phase stability of these two compounds with respect to the diamond phase and their structural and electronic properties under pressure. We have also calculated the active Raman frequencies as well as their pressure dependence as a milestone for future experiments. First, our calculations confirmed the interesting structural properties of these clathrates. In particular, these structures are of low compressibility but are still more compressible than diamond. As a result, no collapse of cell volume with increasing pressure was evidenced as occurs in silicon clathrate in the same studied pressure range. Our calculations for the C_{46} clathrate are in a good agreement with previous studies. In the case of Li_8C_{46}, we find a large enthalpy at zero pressure related to diamond. Furthermore, the Li-intercalated clathrate becomes the stable phase relative to diamond near −187 GPa, pointing to a difficulty in synthesizing this compound. We have also proposed a reaction path involving stoichiometric ratios of diamond and lithium to obtain the Li_8C_{46}. Although this reaction seems not be favorable, we have calculated a minimum corresponding to an energy barrier of approximately 1.9 eV around 38–39 GPa, an easily accessible pressure-window with the diamond anvil cell. Hence, even if the phase stability of Li_8C_{46} appears to be a serious obstacle, our result leads us to suppose that HPHT conditions are well suited to obtaining this compound. *Ab initio* cannot provide a synthesis route; future attempts may allow us to find it. Further *ab initio* calculations on intercalated clathrates considering other chemical species or with different structures will be valuable in order to reduce the cohesive energy.

Acknowledgments

This work was made possible through the financial support of the Spanish–French Picasso Program. PR-H and AM acknowledge the financial support of the Spanish MEC under grants MAT2004-05867-C03-03 and MAT2007-65990-C03-03. NR wishes to thank S Radescu and A Mujica for fruitful discussions.

References

[1] Nesper R, Vogel K and Blöchl P E 1993 Hypothetical carbon modifications derived from zeolite frameworks *Angew. Chem. Int. Edn Engl.* **32** 701–3
[2] Saito S 1997 Electronic structure of covalent-bond clusters and materialsdesign *Proc. 1st Symp. on Atomic-scale Surface and Interface Dynamics*
[3] Blase X, Gillet P, San Miguel A and Melinon P 2004 Exceptional ideal strength of carbon clathrates *Phys. Rev. Lett.* **92** 215505
[4] Connétable D *et al* 2003 Superconductivity in doped sp^3 semiconductors: the case of the clathrates *Phys. Rev. Lett.* **91** 247001
[5] Timoshevskii V, Connetable D and Blase X 2002 Carbon cage-like materials as potential low work function metallic compounds: case of clathrates *Appl. Phys. Lett.* **80** 1385–7
[6] Iqbal Z *et al* 2003 Evidence for a solid phase of dodecahedral c-20 *Eur. Phys. J.* B **31** 509–15
[7] Piskoti C, Yarger J and Zettl A 1998 C-36, a new carbon solid *Nature* **393** 771–4
[8] Ker A, Todorov E, Rousseau R, Uehara K, Lannuzel F X and Tse J S 2002 Structure and phase stability of binary zintl-phase compounds: lithium group 13 intermetallics and metal-doped group 14 clathrate compounds *Chem. Eur. J.* **8** 2787–98
[9] Saito S and Oshiyama A 1995 Electronic structure of Si_{46} and $Na_2Ba_6Si_{46}$ *Phys. Rev.* B **51** 2628–31
[10] Bernasconi M, Gaito S and Benedek G 2000 Clathrates as effective p-type and n-type tetrahedral carbon semiconductors *Phys. Rev.* B **61** 12689–92
[11] Spagnolatti I, Bernasconi M and Benedek G 2003 Electron–phonon interaction in carbon clathrate hex-c-40 *Eur. Phys. J.* B **34** 63–7
[12] Zipoli F, Bernasconi M and Benedek G 2006 Electron–phonon coupling in halogen-doped carbon clathrates from first principles *Phys. Rev.* B **74** 205408
[13] San-Miguel A, Kéghélian P, Blase X, Mélinon P, Perez A, Itié J P, Polian A, Reny E, Cros C and Pouchard M 1999 High pressure behavior of silicon clathrates: a new class of low compressibility materials *Phys. Rev. Lett.* **83** 5290–3
[14] Yamanaka S, Enishi E, Fukuoka H and Yasukawa M 2000 High-pressure synthesis of a new silicon clathrate superconductor, Ba_8Si_{46} *Inorg. Chem.* **39** 56–8
[15] Yamanaka S, Kubo A, Inumaru K, Komaguchi K, Kini N S, Inoue T and Irifune T 2006 Electron conductive three-dimensional polymer of cuboidal C_{60} *Phys. Rev. Lett.* **96** 076602
[16] San-Miguel A and Toulemonde P 2005 High-pressure properties of group IV clathrates *High Pressure Res.* **25** 159–85
[17] Mao W L, Mao H K, Eng P J, Trainor T P, Newville M, Kao C C, Heinz D L, Shu J F, Meng Y and Hemley R J 2003 Bonding changes in compressed superhard graphite *Science* **302** 425–7
[18] Vienna *ab initio* package, for more information please see http://www.cms.mpi.univie.ac.at/vasp
[19] Blöchl P E 1994 Projector augmented-wave method *Phys. Rev.* B **50** 17953–79
[20] Kresse G and Joubert D 1999 From ultrasoft pseudopotentials to the projector augmented-wave method *Phys. Rev.* B **59** 1758–75

[21] Perdew J P, Burke K and Ernzerhof M 1996 Generalized gradient approximation made simple *Phys. Rev. Lett.* **77** 3865–8
[22] Lee I-H and Martin R M 1997 Applications of the generalized-gradient approximation to atoms, clusters, and solids *Phys. Rev.* B **56** 7197–205
[23] Janotti A, Wei S-H and Singh D J 2001 First-principles study of the stability of BN and C *Phys. Rev.* B **64** 174107
[24] Murnaghan F 1944 *Proc. Natl Acad. Sci. USA* **30** 244
[25] McSkimin H J and Andreatch P Jr 1972 Elastic moduli of diamond as a function of pressure and temperature *J. Appl. Phys.* **43** 2944–8
[26] Madelung O (ed) 1991 *Landolt–Bornstein Group III Condensed Matter. Data in Science and Technology. Semiconductors: Group IV and III–V Compound* (Berlin: Springer)
[27] Adams G B, O'Keeffe M, Demkov A A, Sankey O F and Huang Y-M 1994 Wide-band-gap Si in open fourfold-coordinated clathrate structures *Phys. Rev.* B **49** 8048–53
[28] Benedek G, Galvani E, Sanguinetti S and Serra S 1995 Hollow diamonds—stability and elastic properties *Chem. Phys. Lett.* **244** 339–44
[29] O'Keeffe M, Adams G B and Sankey O F 1998 Duals of Frank–kasper structures as C, Si and Ge clathrates: energetics and structure *Phil. Mag. Lett.* **78** 21–8
[30] Perottoni C A and da Jornada J A H 2001 The carbon analogues of type-I silicon clathrates *J. Phys.: Condens. Matter* **13** 5981–98
[31] Adams G B, Sankey O F, Page J B, O' Keeffe M and Drabold D A 1992 Energetics of large fullerenes—balls, tubes, and capsules *Science* **256** 1792–5
[32] San-Miguel A, Mélinon P, Connétable D, Blase X, Tournus F, Reny E, Yamanaka S and Itié J P 2002 Pressure stability and low compressibility of intercalated cagelike materials: the case of silicon clathrates *Phys. Rev.* B **65** 054109
[33] San-Miguel A *et al* 2005 Pressure-induced homothetic volume collapse in silicon clathrates *Europhys. Lett.* **69** 556–62
[34] Yang L *et al* 2006 Pressure-induced phase transformations in the Ba_8Si_{46} clathrate *Phys. Rev.* B **74** 245209
[35] Dong J and Sankey O F 1999 Theoretical study of two expanded phases of crystalline germanium: clathrate-I and clathrate-II *J. Phys.: Condens. Matter* **11** 6129–45
[36] Blase X 2003 Quasiparticle band structure and screening in silicon and carbon clathrates *Phys. Rev.* B **67** 035211
[37] Parlinski K 2003 Phonon software http://wolf.ifj.edu.pl/phonon/
[38] Alfè D 1998 Program available at http://chianti.geol.ucl.ac.uk/~dario
[39] Kresse G, Furthmuller J and Hafner J 1995 *Ab initio* force constant approach to phonon dispersion relations of diamond and graphite *Europhys. Lett.* **32** 729–34
[40] Alfè D, Price G D and Gillan M J 2001 Thermodynamics of hexagonal-close-packed iron under earth's core conditions *Phys. Rev.* B **64** 045123
[41] Connetable D and Blase X 2004 Electronic and superconducting properties of silicon and carbon clathrates *Appl. Surf. Sci.* **226** 289–97